



Research Paper

Effect of Non-Solvent Additives to the Casting Solution on the Structure and Properties of Polyethersulfone UF Membranes

Alexandr Bilydukevich ¹, Tatsiana Hliavitskaya ^{1,*}, Galina Melnikova ²¹ Institute of Physical Organic Chemistry, National Academy of Sciences of Belarus, 13 Surganov Street, Minsk 220072, Belarus² The A. V. Luikov Heat and Mass Transfer Institute, National Academy of Sciences of Belarus, 15 P. Brovki Street, 220072 Minsk, Belarus

Article info

Received 2020-03-26

Revised 2020-05-08

Accepted 2020-05-13

Available online 2020-05-13

Keywords

Phase inversion
 Polyethersulfone (PES)
 Non-solvent additive effect
 Precipitation value
 Degree of saturation

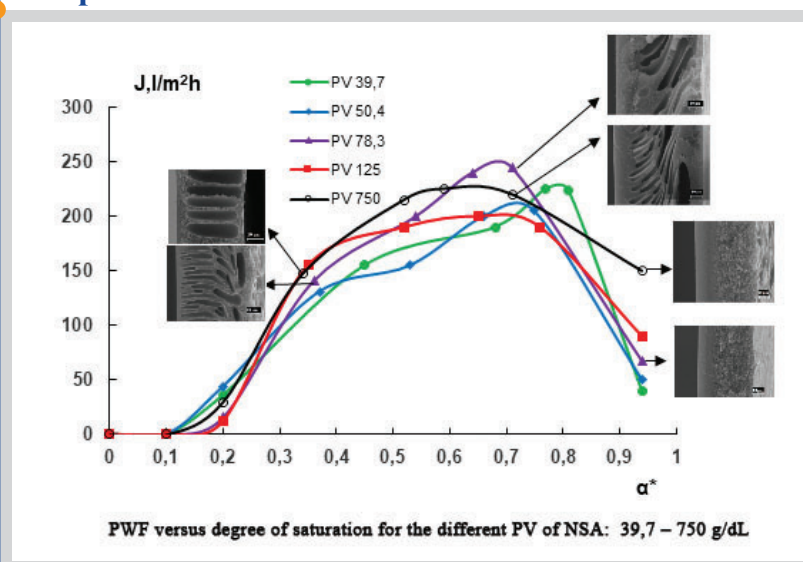
Highlights

- Structure and properties of UF membranes depend on the precipitation value of NSA
- The higher the PV of NSA, the higher PWF of membranes with the spongy structure
- Membranes with max. performance are obtained when $\alpha^* = 0.52 - 0.81$

Abstract

The obtained results in this work allow us to propose a new approach to fabricate polyethersulfone (PES) ultrafiltration (UF) membranes with desired structure and performance. It was shown that UF membranes with a spongy structure are obtained from casting solutions located near the binodal line. However, with increasing the precipitation value (PV) of non-solvent additives (NSA), the higher pure water flux (PWF) of membranes with the spongy structure was observed. UF membranes with maximum performance are obtained when degree of saturation (α^* – the ratio of the NSA amount added to the polymer solution to the NSA amount which causes phase separation) $\alpha^* = 0.52 - 0.81$ (depending on PV of NSA). In this case, macrovoids will prevail in the structure of the supporting layer of membranes. The size and shape of macrovoids also depend on the PV of NSA. The higher the PV of NSA, the larger the size of macrovoids in the structure of supporting layer.

Graphical abstract



© 2021 MPRL. All rights reserved.

1. Introduction

Polyethersulfone (PES) is widely used as a membrane-forming polymer owing to its high chemical resistance, thermal stability, remarkable mechanical properties and the relative simplicity of the membrane production in various configurations. Main technique of PES membrane preparation is a phase separation method in various modifications such as non-solvent induced phase separation (NIPS), thermally induced phase separation (TIPS), vapor induced phase separation (VIPS), and evaporation induced phase separation (EIPS) [1-3]. The NIPS process is implemented by precipitation of a homogeneous polymer solution in a coagulation bath (typically water or water-non-solvent mixture) and is the most widely used technique for the preparation of PES ultrafiltration membranes [4]. The main requirement for casting solution is its homogeneity; i.e., the composition of the solution on the polymer/solvent/non-solvent ternary phase diagram must be located in the miscibility region [1-5]. Membranes that are prepared by the NIPS process usually contain

large elongated voids (macrovoids) in their sublayer structure. The type and structure of these macrovoids significantly affects the performance and mechanical strength of the resulting membranes. It is noted [6,7] that macrovoids is an undesirable phenomenon and their presence can lead to the damage of the membrane selective layer under the pressure applied. The non-solvent additive (NSA) to the casting solution is the widely used procedure to suppress the macrovoid formation and improve the membrane permeability. Membranes obtained from casting solutions including non-solvent additives usually have a spongy structure in the cross-section without macrovoids [6,8-11]. The wide range of compounds can be used as NSA in casting solution: water, mono- and polyhydric alcohols, glycols, organic acids, etc., as well as mixtures of various non-solvents [12-21]. NSA strongly affects the casting solution viscosity and kinetics of phase separation and therefore morphology and performance of the resulting

* Corresponding author: thliavitskaya@gmail.com (T. Hliavitskaya)

membranes [6,14,22-25]. NSA introduction in the casting solution renders the casting composition closer to binodal on polymer/solvent/non-solvent phase diagram and is one of the key approaches to regulating the membrane structure, including the control of macrovoids formation, and membrane permeability [9,26].

There are several approaches to estimate the position of casting solution composition relative to the binodal curve on ternary phase diagram polymer/solvent/non-solvent. Some authors use the approaching ratio (α) which is defined as weight ratio of non-solvent and solvent in the casting solution to weight ratio of non-solvent and solvent at the cloud point [27-30]. In [29] the degree of saturation (α^*) (the ratio of the NSA amount added to the polymer solution to the NSA amount which causes phase separation) is used for characterization of the casting solution composition. As will be shown below, both approaches give comparable results. Liu et al. [6] proposed the ratio of water added and amount of water required to reach phase separation to characterize the casting solution and defined this ratio as a coagulation value (%). Wang et al. [31-33] proposed the term "precipitation ratio" ($R_{a/s}$) to characterize the composition of casting solutions. The $R_{a/s}$ is defined as the ratio of the weight of non-solvent additive to the weight of solvent (w/w) in the casting solution, although the use of this parameter seems to be rather questionable, as it does not provide any information about the position of the casting solution on the ternary phase diagram.

It should be noted that different non-solvents have different affinity to the polymer and affect the miscibility region area (binodal position) on the ternary phase diagram as well as the viscosity of polymer solutions [6,22-24, 30]. For characterization of NSA in casting solution as well as for evaluating the effect of composition of the coagulation bath on the structure and performance of membranes the precipitation value (PV) or coagulation value (CV) is used [25,34-41]. In chemical fiber science precipitation value is determined as the non-solvent amount (in grams) which causes clouding of 100 ml of 1 wt.% polymer solution (g/dL). PV is used to characterize the power of a coagulation bath towards the polymer/solvent system [34,41,42]. Wang et al. [31-33] determined PV as the quantity of non-solvent required to make a polymer solution containing 2 g of polymer and 100 g of solvent turbid in order to choose the composition of casting solution and select the suitable non-solvent as a coagulation bath.

In contrast to PV there are significant methodological differences in determination of coagulation value: different concentration and volume of polymer solution are used in literature and, therefore, different CV units are obtained. Lai et al. [37] measured CV by titration polymer solution containing 1 g of polymer poly(4-ethyl-1-pentene), 23,75 ml of cyclohexane and 3,75 ml of different NSA using ethanol. Titration was carried out at 40°C. The membrane porosity was found to decrease with the increase in the coagulation value [37]. Feng et al. [24] used CV to characterize the thermodynamic stability of 26% casting solutions based on sulfonated polyphenylenesulfone containing PEG-400 as additive. In this case, the coagulation value is defined as the amount of water (coagulant) in grams, which causes the phase separation of 10 g of casting solution. The decrease in the CV due to the addition of PEG-400 into the casting solution leads to the formation of asymmetric membranes with a thin skin layer and suppresses macrovoid formation in the membrane substructure, which is attributed to the accelerated kinetics of phase separation process [24]. The effect of acetone, ethanol and water as a coagulant on the structure and properties of ethylene-vinyl alcohol copolymer (EVAL) membranes was studied by Chen et al. [38] by comparing CV of different non-solvents. Non-solvents were added to a 15 wt.% EVAL solution at 25°C until the first permanent coagulation was obtained. The different DMAc/water mixtures were tested as coagulants by Chun et al. [40] by titration of 6,5 ml 2 wt.% polyimide solutions until the solution became milky-white, which confirmed that the phase separation occurred. The amount of added coagulant was recorded as the coagulation value. It was found out that the CV increase of non-solvent in a coagulation bath results in a decrease of specific pore volume of the membranes.

It can be concluded that the "coagulation value" (CV) is an analog of the "precipitation value" (PV). As a rule, PV or CV describes the phase separation process in the region of low polymer concentrations (<2%) and does not provide any information on the behavior of concentrated polymer solutions used for membrane fabrication. Wang et al. [32] tried to establish the relationship between the CV and the precipitation ratio $R_{a/s}$ for (PES)/N-methylpyrrolidone (MP)/methanol (MeOH), polysulfone (PSf)/DMAc/MeOH, PES/MP/H₂O, PSf/DMAA/H₂O and other systems. An equation for prediction of the composition of casting solution containing NSA was proposed. The satisfactory accordance between calculated and experimental data for 2% PES of PSf solutions in MP and DMAc was shown.

The objective of this study is to establish the correlation between NSA precipitation value and the structure and performance of ultrafiltration membranes. As it was mentioned above, the introduction of NSA to the casting solution brings the composition closer to binodal (precipitation point).

In this case, if the same coagulation bath is used in NIPS process, the coagulant tolerance of membrane casting solution decreases upon addition of NSA. There is an important factor related to casting solution composition, which effects membrane structure and performance: tolerance of the casting solution toward the coagulant. Zheng et al. [43] define coagulant tolerance as actual non-solvent proportion, which lead to membrane precipitation. In order to exclude the influence of the casting solution tolerance towards the coagulant on the membrane structure and performance the casting solutions with a fixed value of the degree of saturation ($\alpha^*=0.94-0.95$) were used in this study. According to the literature review the effect of NSA power to casting solution (such parameters as PV and CV) on the properties and structure of membranes haven't been studied yet. This is due to the differences in methodological approaches. Moreover, the position of the casting solution composition on the phase diagram towards the binodal is not taken into account, i.e., α^* of the casting solution. At the same time, the NSA affinity to the polymer/solvent system determines the temperature-concentration stability of polymer casting solutions and their viscosity, which greatly affects kinetics of phase separation and properties of the resulting membranes.

2. Experimental

2.1. Materials

Polyethersulfone (Ultrason E 6020P) was purchased from BASF, Germany. N,N-dimethylacetamide (DMAc, BASF, Germany) was used as the solvent, distilled water, 85% phosphoric acid, glycerol (QREC) and polyethylene glycol $<M_n> = 400$ g·mol⁻¹ (PEG-400, BASF, Germany) were used as NSA to the casting solutions. Distilled water was used as coagulant. Polyvinylpyrrolidone K-30 ($M_n=40000$ g·mol⁻¹, PVP K-30) was purchased from BASF.

2.2. Membrane preparation

The preparation of 22 wt.% PES casting solutions with DMAc as solvent and PEG-400/Glycerol mixtures as NSA was carried out at 90 °C, preparation time was 4 hours. The amount of NSA for the introduction into the casting solution was calculated as NSA which causes phase separation of 22 wt.% PES solution multiplied by the degree of saturation (α^*). Degree of saturation were in range of 0-0.95. Approaching ratio (α) was determined as the weight ratio of NSA and solvent in the casting solution to weight ratio of NSA and solvent in the cloud point.

The membranes were prepared by the non-solvent induced phase inversion method. The polymer solutions were cast on a glass plate in a uniform thickness of about 200µm. The glass plates were immersed immediately into distilled water as coagulation bath ($T=23$ °C) to induce the phase inversion. The formed membranes were washed two times by distilled water and kept for 24 hours in distilled water to remove the traces of solvent and then were placed in 30% glycerol aqueous solution to prevent pore contraction.

2.3. Precipitation value measurements

The precipitation value (PV) was determined by titration of 100 ml of 1 wt.% PES solution in DMAc by individual non-solvents and their mixtures with PEG-400 in various mass ratios until the solution became visibly turbid. PV expressed in g/dL.

2.4. Membrane characterization

Pure water flux (J , l/m²h) is determined by the ratio:

$$J = \frac{V}{S \cdot t} \quad (1)$$

where V is the volume of permeate (l); S is the area of the working surface of the membrane (m²); t is the filtration time (h).

The rejection of polyvinylpyrrolidone K-30 was calculated using the following equation:

$$R = \left(1 - \frac{C_p}{C_f}\right) \cdot 100\% \quad (2)$$

where C_p - concentration of PVP in the permeate, (g/l); C_f - concentration of PVP in the feed solution, (g/l).

The morphology (surface and cross-section) of the membranes was

studied by using scanning electron microscope LEO 1420, after cryogenic fracture in liquid nitrogen, followed by deposition of a gold layer by cathode sputtering in an EMITECH K 550X vacuum unit (Germany).

The structure of membrane selective layer was studied by atomic force microscopy (AFM, NT-206, Mikrotestmashines, Belarus). Standard silicon cantilevers (NSC35, Mikromasch, Estonia) with a rigidity 3,5 N/m (according to the manufacturer's passport) were used for this study.

3. Results and discussion

3.1. Selection of non-solvent additive

As potential NSA (with different PV) for PES/DMAc solution the weak non-solvent – PEG-400 (PV>1000 g/dL) and stronger non-solvents: water (PV = 10.6 g/dL), 85% phosphoric acid aqueous solution (PV = 13.0 g/dL), glycerol (PV = 27.8 g/dL), as well as mixtures of weak and strong non-solvents in various ratios were used. The plots of PV versus PEG-400/water, PEG-400/phosphoric acid and PEG-400/Glycerol mixtures are shown in Figure 1. It can be seen that PV of studied mixtures vary over a wide range: from 15 to 1000 g/dL. The PV dependence on PEG-400 concentration in the mixture features non-additive character. The effect of a strong non-solvent (water, phosphoric acid) on PV prevailed up to a PEG-400 concentration of 80 wt.% and only after that the sharp increase in PV concentration was observed, which indicated the decrease in the non-solvent power of these non-solvent mixtures. When PEG-400/Glycerol mixtures are used, the PV dependence on the concentration of PEG-400 is not as sharp as in case of PEG-400/water or PEG-400/H₃PO₄ mixtures and allows changing the PV of the NSA in a wide range. According to the results the obtained PEG-400/Glycerol mixtures with the following mass ratio of the components were used for further studies: 0/100 (PV=27.8 g/dL), 15/85 (PV=39.7 g/dL), 30/70 (PV=50.4 g/dL), 50/50 (PV =78.3 g/dL), 60/40 (PV = 125 g/dL), 70/30 (PV = 250 g/dL), 80/20 (PV =750 g/dL).

3.2. Effect of PV of NSA on the properties of casting solutions

Figure 2 shows the maximum concentration dependence of PEG-400/Glycerol mixtures in 22 wt.% PES solution on PV of NSA. It can be seen, that the increase in PV of NSA (decrease in non-solvent power) leads to the increase in its concentration, at which it is possible to get stable homogeneous solutions. Thus, the maximum concentration of glycerol (PV = 27.8 g/dL) is 17 wt.%, for PEG-400/Glycerol =15/85 mixture with PV = 39.7 g/dL – 18.7 wt.%, for PEG-400/Glycerol = 20/80 mixture (PV=750 g/dL) – 40wt.%, and in case of pure PEG-400 the homogeneous and kinetically stable solution can be obtained up to 60 wt.% of the PEG concentration.

The results of the viscosity measurements of PES solutions with PEG-400/Glycerol mixtures are shown in Figure 3. It was established that at a constant NSA concentration a decrease in PV of non-solvent leads to the increase in the dynamic viscosity of the PES solutions. When the concentration of NSA in the casting solution was 15 wt.%, the viscosity of the solutions increases gradually with decreasing of the non-solvent PV: for the mixture with PV = 750 g/dL the viscosity was 3.78 Pa·s, for PV = 78.3 g/dL – 5.15 Pa·s, and for PV=50.4 g/dL – 6.05 Pa·s. However, when the weak non-solvents (with PV > 80 g/dL) are used it can be possible to increase the concentration of NSA without the phase separation of the solution and adjust the viscosity of casting solutions within the wide range. Thus, when increasing the concentration of the PEG-400/Glycerol mixture with PV=750 g/dL from 15 to 40 wt.%, the viscosity of the solution increases from 3.78 to 27.5 Pa·s.

3.3. Effect of PV of NSA on membrane performance

The membranes were fabricated from four-component PES/PEG-400/Glycerol/DMAc solutions with the degree of saturation (α^*) in the range of 0-0.95 for different PV of NSA (39.7-750 g/dL). PES concentration was constant – 22 wt.%. Concentration of 22 wt.% was selected specially, since the dependence of membrane pure water flux (PWF) on the PES content indicates that the films which were obtained from a 22 wt.% PES-DMAc solutions were completely impermeable to water.

The composition of the mixture PEG-400/Glycerol influences on the position of binodal line (see Figure 2). At the same time amount of the PEG-400/Glycerol mixtures in the polymer solution influence on the position of final composition of casting solution relative to the binodal line. In essence, amount of the PEG-400/Glycerol mixtures in the casting solution influence on the quantity of the non-solvent that can be added to the casting solution before the phase separation occur. In order to obtain comparable results (to evaluate

effect of PV of NSA on membrane performance), compositions of the casting solutions were specially selected in such a way that they feature the degree of saturation (α^*) in the range of 0.94-0.95, i.e. the compositions of casting solutions should be located (fixed) near the binodal. These casting solution compositions are listed in Table 1. This value of α^* was chosen specially to suppress the macrovoid formation in the membrane supporting layer [8]. The comparison of α^* values and the approaching ratio (α) showed that they have similar values. The approaching ratio values are usually 2-5% lower than the degree of saturation.

Figure 4 shows the dependence of pure water flux of membranes (J) and PVP K-30 rejection (R) on the PV of PEG-400/Glycerol mixtures. According to Figure 4, the increase in PV of NSA leads to the increase of pure water flux of membranes. The sharpest increase in the pure water flux of membranes was observed in the range of PV 39.7-125 g/dL, thereafter the increase in the pure water flux of membranes wasn't so significant. It was found that decrease in PV of NSA leads to the decrease in the rejection of the PVP K-30 from 93 down to 85%. Increase in pure water flux of membranes with an increase in PV of NSA apparently associated with changes in the supramolecular structure of polymer solutions, which affects the kinetics of phase separation process [44,45].

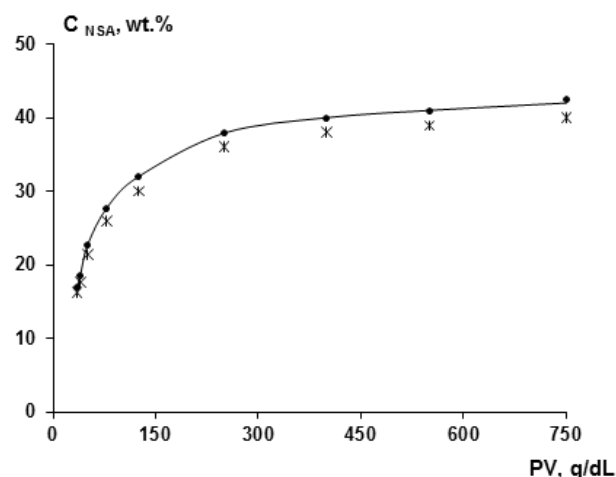


Fig. 2. Dependence of NSA concentration for 22 wt.% PES solution at the cloud point on PV of PEG-400/Glycerol mixtures. Star-shaped markers indicate the compositions used for membranes formation.

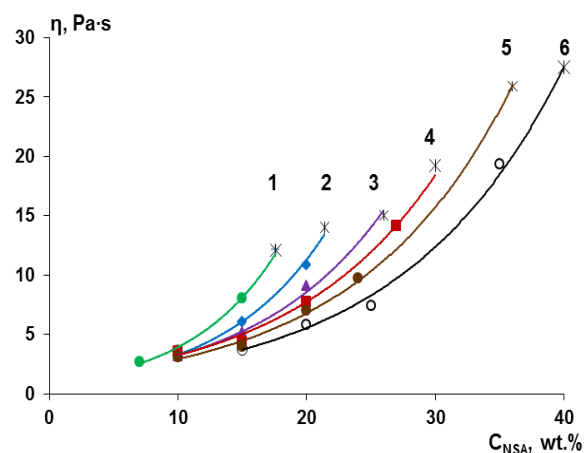


Fig. 3. Viscosity of 22 wt.% PES/DMAc solution vs. the concentration of PEG-400/Glycerol mixtures with different PV: 1 - 39.7 g/dL ; 2 - 50.4 g/dL; 3 - 78.3 g/dL; 4 - 125 g/dL; 5 - 250 g/dL; 6 - 750 g/dL. Star-shaped markers indicate the concentration of PEG-400/Glycerol mixture corresponding to $\alpha = 0.94-0.95$ at 25° C.

Table 1
Compositions of PES casting solutions

Compositions of casting solutions (wt.%)				PV NSA, (g/dL)	degree of saturation α^*	approaching ratio (α)	Viscosity, (Pa·s)
PES	Glycerol	PEG-400	DMAc (wt.%)				
22	15,0	2,6	60,4	39,7	0,95	0,93	12,1
22	14,8	6,6	56,6	50,4	0,94	0,92	14,0
22	13,0	13,0	52,0	78,3	0,94	0,91	14,9
22	12,0	18,0	48,0	125	0,94	0,90	19,2
22	10,8	25,2	42,0	250	0,95	0,89	25,9
22	8,0	32,0	38,0	750	0,94	0,88	27,5

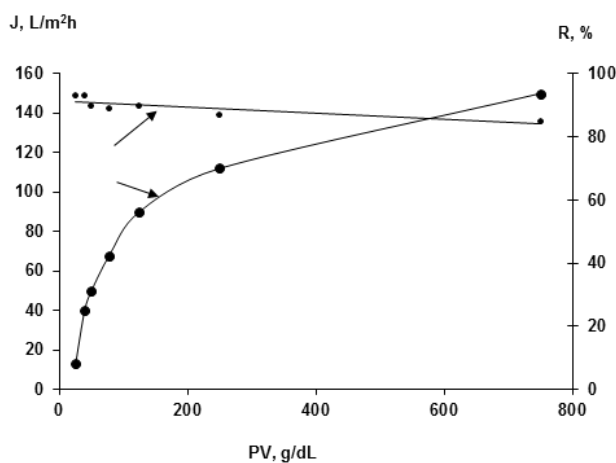


Fig. 4. Dependence of pure water flux of membranes (J) and rejection (R) of PVP (K-30) on the precipitation value (PV) of PEG-400/Glycerol mixtures.

3.4. Effect of PV of NSA on membrane structure

SEM study of the membrane cross section structure showed that membrane morphology does not undergo the significant changes (Figure 5). The structure of all samples can be characterized as follows: a dense selective layer is followed by a more porous sublayer, in its structure the structural elements are well discerned (Figure 5a-d). The sublayer has a sponge-like structure without finger-like macrovoids which is due to the high values of the α^* of the casting solutions. The only difference is the thickness increase of the selective layer with the increase in PV of the NSA. The increase of PV from 39.7 g/dL to 78.3 g/dL was shown to lead to the increase in the thickness of the skin layer from 1 μm to 2.5 μm , and for PV = 750 g/dL the thickness of the skin layer is 4.5 μm . Also, the increase in PV leads to the gradual decrease of the density of membrane porous sublayer. It was found that upon the increase of PV from 39.7 g/dL (Figure 5a) to 750 g/dL the transition from loose spongy structure of the sublayer to denser structure occurs (Figure 5d).

The mechanism of the development of this typical membrane structure was described in [46]. It is assumed that the established regularities (increase of the thickness of the selective layer with the increase in PV of the NSA) are due to the increase in the viscosity of the casting solutions near the binodal line with the increase in PV of the NSA (see Table 1) [14], as well as to the differences in the structure of the selective layer which structure is not detectable even at 20,000-time magnification.

AFM-analysis was used to investigate the surface topography of the membranes. Figure 6 illustrates two and three dimensional AFM images of the PES membranes prepared from casting solutions with different PV of NSA. The brightest areas present the highest point of the membrane surface and dark regions indicate the low spots (valleys). An increase in PV of NSA leads to an increase in the area of the valleys and change in their shape from circular shape to more elongate one. It was shown that the PV of NSA in the casting solution affects the roughness of the membrane surface. Table 2 presents the information how PV of NSA influences the root-mean-squared surface roughness (R_q) and average roughness (R_a) at a scan size of $5 \mu\text{m} \times 5$

μm . R_a and R_q increased from 6.4 to 41.9 and 8.2 to 58.0 respectively while PV of NSA in casting solution rose from 39.7 up to 750 g/dL. An increase in R_a and R_q is associated with an increase of surface heterogeneity.

The obtained results allow us to explain the existing contradiction in the scientific literature. A number of authors postulate that when the composition of the casting solution was located near the binodal line, high-performance membrane structures was obtained. Another range of authors contrary consider that membranes with very low PWF were obtained from the casting solution located near the binodal. In particular, Kim and Lee [48] postulated that membranes prepared from solutions with higher ratio of non-solvent to solvent (PEG-600/NMP) i.e. from solutions with higher degree of saturation (approaching ratio) have higher PWF. Results of Kim can be explained by a high PV of PEG-600 >> 1000 g/dL. In case of membranes prepared from dope solutions containing rather strong NSA low PWF might be explained by lower PV. In this case, the results of Sinha and Purkait work are rather indicative [49]. The dependence of membrane PWF against concentration of NSA (methanol) was extreme. The minimum PWF was observed at the maximum concentration of NSA in the polymer solution. The existing contradiction (relatively high and low PWF of membranes prepared from polymer/non-solvent/solvent solutions located near the binodal line) is explained by the difference in PV of NSA. For strong NSA - PWF is low, for weak NSA - PWF is high.

3.5. Correlation between PV of NSA, degree of saturation (α^*), and membrane properties

Properties of membranes cast from polymer solutions located near the binodal line ($\alpha^* = 0.94-0.95$, PV of NSA 39.7-750 g/dL) were discussed above. At the same time, it is interesting how PV of NSA affects membrane properties in a wide range of the degree of saturation ($\alpha^* = 0-0.95$). The dependence of membrane PWF on PV of NSA for different degrees of saturation of casting solutions is presented on Figure 7. Membranes obtained from PES/PEG-400/Glycerol/DMAc solution with $\alpha^* = 0 - 0.1$ are impermeable to water at 1 bar. Further increase in α^* up to 0.59-0.81 led to an increase in membrane PWF. Near the binodal line ($\alpha^* = 0.94-0.95$) membranes PWF decreased again. The dependences of membrane PWF on the degree of saturation of casting solution are found to be extreme (pass through the maximum). These results agree with the earlier data reported in [36,49]. In case of strong NSA (with low PV) there is a tendency towards to more extreme dependence PWF vs. α^* , in comparison with weak NSA (with greater PV). When PV of NSA ≤ 78.4 g/dL the difference between the maximum PWF and PWF of membranes cast from solution with $\alpha^* = 0.94-0.95$ was 150-185 l/m²h. In case of PV of NSA ≥ 150 g/dL this difference was not so significant - 75-100 l/m²h. Maximum PWF is observed in the case of membranes obtained from casting solutions with $\alpha^* = 0.59-0.81$ (depending on PV of NSA). Figure 8 presents the degree of saturation that corresponds to the maximum PWF ($\alpha^*(J_{max})$) plotted against the PV of NSA in the casting solution. As follows from Figure 8, as PV of NSA increases, the degree of saturation that corresponds to the maximum PWF decreased.

Figure 9 shows how the membrane structure transforms with an increase in degree of saturation of casting solutions in case of rather strong NSA (PV = 78.3 g/dL) and in case of weak NSA (PV = 750 g/dL). Figure 9a presents the cross section structure of membrane which was prepared from the casting solution without NSA ($\alpha^* = 0$). In the structure of the membrane supporting layer, a lot of macrovoids were observed, which significantly differ in their size. It was found that the increase in degree of saturation of casting solution up to 0.35-0.36 leads to the formation of the sponge-type structure between skin and supporting layer (see Figure 9 b and c). At this degree of saturation of the casting solutions, the difference in PV of NSA also affects the

membrane structure. In case of weak NSA (PV=750 g/dL) macrovoids were located along the entire length of the supporting layer of membranes. When PV of NSA = 78.3 g/dL, the size of macrovoids was not so huge. Supporting layer of these membranes was shown to feature so called a finger-like structure. A similar situation is observed in the case of $\alpha^*=0.71-0.72$. For different PV of NSA, the difference in the number of macrovoids and their sizes is recorded. Macrovoids in the supporting layer can be initiated by non-homogeneous demixing on the border non-solvent – casting solution, which is

favoured by dynamic fluctuation caused by rapid exchange between DMAc (solvent) and water (non-solvent) [46,47]. Sizes of macrovoids apparently depends on PV of NSA as well as on rheological property of the casting solution. A subsequent increase in the degree of saturation to 0.94 led to the disappearance of macrovoids and formation of completely spongy structures (Figure 9 f and g). The differences of these structures from each other were discussed above.

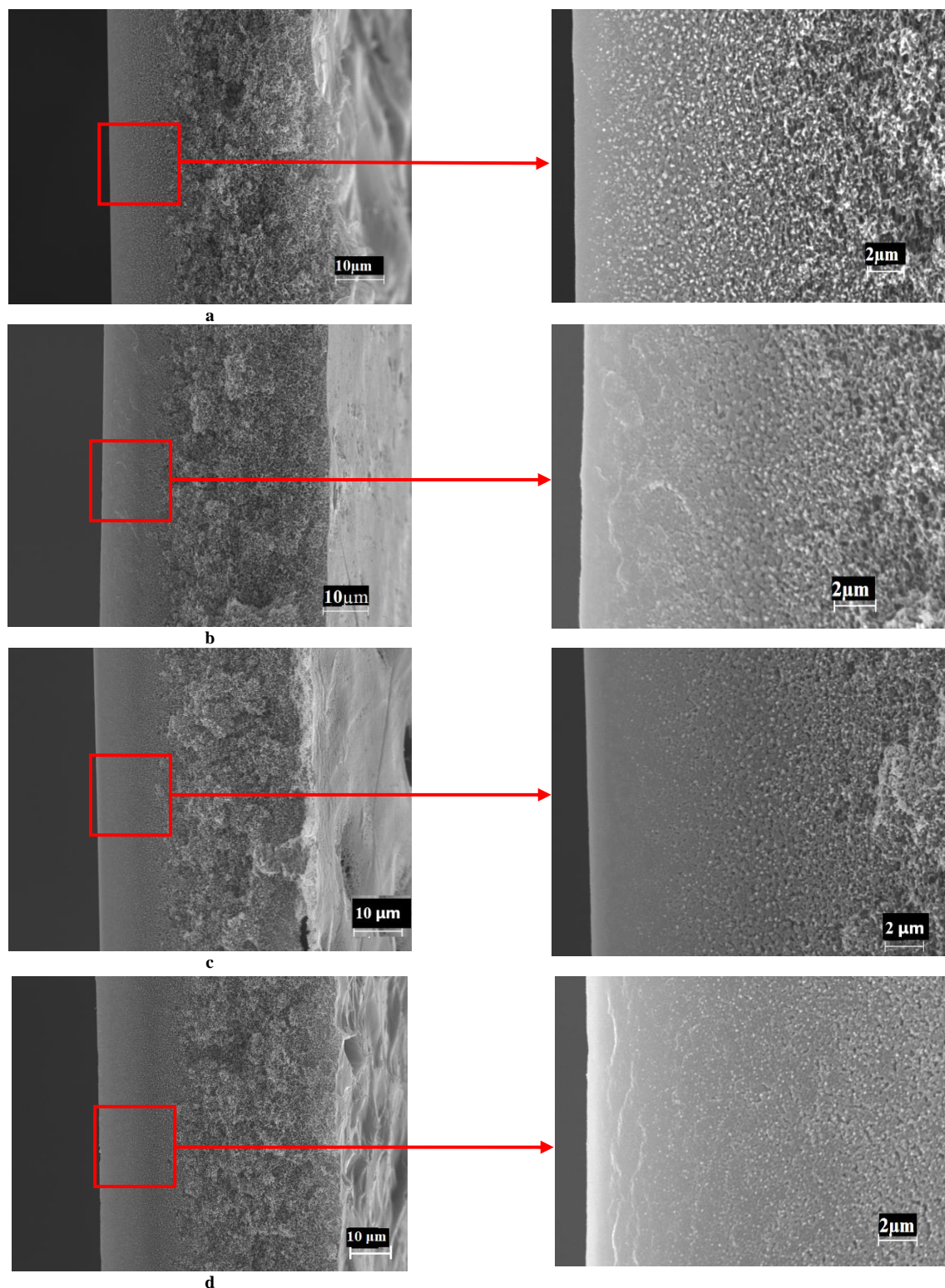


Fig. 5. Scanning electron micrographs of the cross section structure of PES membranes prepared from a casting solutions with PEG-400/Glycerol mixtures with different PV: a - 39.7 g/dL; b - 78.3 g/dL; c - 125 g/dL; d - 750 g/dL.

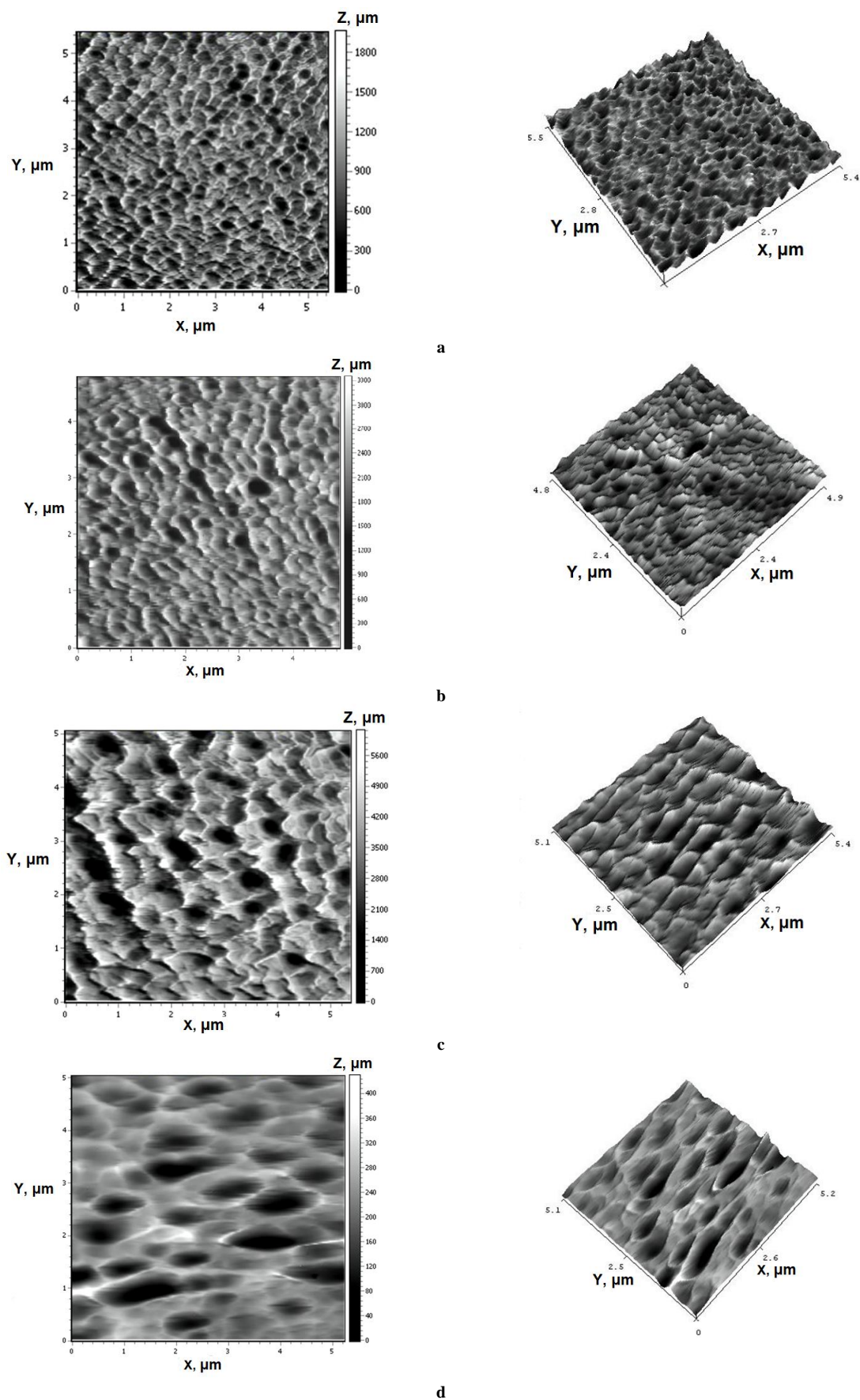


Fig. 6. The AFM images of the selective layer of PES membranes. PV of NSA: (a) 37.9 g/dL; (b) 50.4 g/dL; (c) 78.3 g/dL; (d) 750 g/dL.

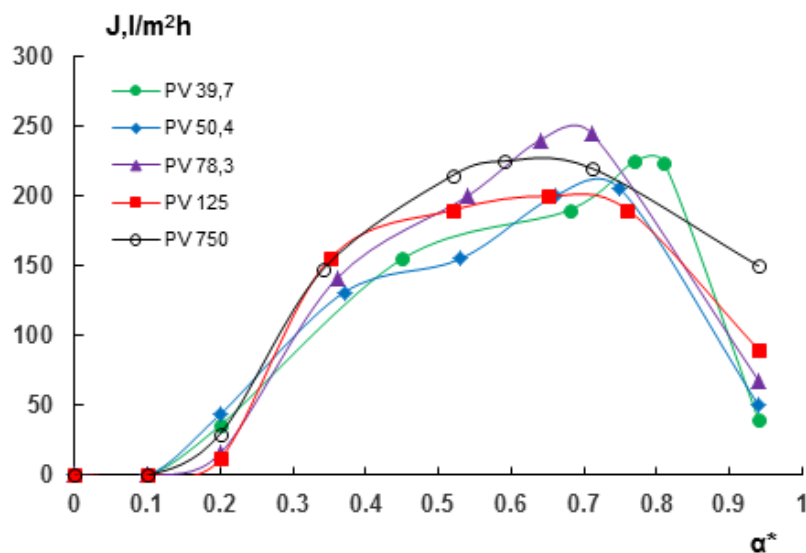


Fig. 7. PWF versus degree of saturation for the different PV of NSA: 39.7 – 750 g/dL.

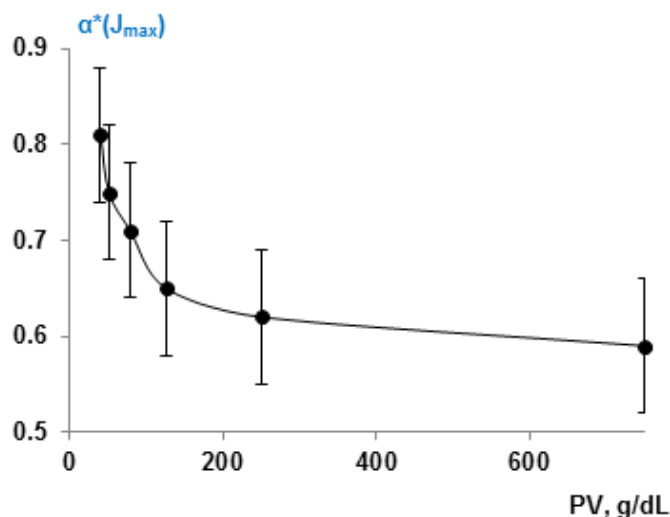


Fig. 8. Dependence of the degree of saturation that corresponds to the maximum PWF ($\alpha^*(J_{max})$) on PV of NSA in casting solution.

The obtained results allow us to propose a new approach to production of membranes with necessary structure and performance. It was shown that membranes with a spongy structure are obtained from casting solutions located near the binodal line. However, the higher the PV of NSA, the higher PWF of membranes with the spongy structure. Membranes with maximum performance are obtained when $\alpha^*=0.52-0.81$ (depending on PV of NSA). In this case, macrovoids will prevail in the structure of the supporting layer of membranes. The size and shape of macrovoids also depend on the PV of NSA. The higher PV of NSA, the larger the size of macrovoids in the structure of supporting layer.

4. Conclusions

The effect of the precipitation value (PV) of mixtures of strong and weak non-solvent additives (NSA) on the phase state and viscosity of polyethersulfone (PES)/N,N-dimethylacetamide (DMAc)/NSA solutions and on the structure and performance of PES membranes were studied. PV of NSA was determined as the non-solvent amount which causes clouding of 100 ml of 1wt.% polymer solution. Polyethylene glycol 400 (PEG-400, PV>

1000 g/dL), water (PV = 10.6 g/dL), 85% phosphoric acid (PV = 13.0 g/dL), glycerol (PV = 27.8 g/dL) and mixtures thereof were used as NSA for PES-DMAc solutions. To vary the PV of NSA in range of 27.8-750 g/dL mixtures of strong (glycerol) and weak (PEG-400) non-solvents were used. Using PEG-400/Glycerol mixtures it was established that the increase of PV of NSA leads to the increase of the miscibility gap on the ternary phase diagram PES/DMAc/NSA. At a constant NSA concentration a decrease in PV of NSA leads to an increase in the dynamic viscosity of the PES solutions. PES flat sheet membranes were fabricated from 22 wt.% casting solutions containing PES, DMAc and PEG-400/Glycerol mixtures as NSA with different PV. In order to exclude the influence of the casting solution tolerance toward coagulant on the membrane structure and performance the casting solutions with a fixed value of the degree of saturation ($\alpha^*=0.94-0.95$) were used in this study. This value of α^* was chosen specially to suppress the macrovoid formation in the membrane supporting layer. For a constant α^* increase in PV of NSA leads to increase of the membrane pure water flux (PWF) from 13 up to 150 l/m²h at 1 bar. The most dramatic increase in PWF was found to occur in the range of PV 39.7-125 g/dL. It was shown that the rejection of PVP K-30 slightly decreases. The SEM studies of membrane structure does not reveal significant differences in the cross-section morphology of membranes for

different PV of NSA (for $\alpha^*=0.94-0.95$). However, AFM analysis reveals a difference in the skin layer structure of membranes. It was noted that the root-mean-squared surface roughness and average roughness increased from 6.4 up to 41.9 and 8.2 to 58.0 respectively when PV of NSA rises from 39.7 up to 750 g/dL. Thus, these studies allow us to conclude that the structure and properties of ultrafiltration membranes strongly depend on the precipitation value of NSA but not only on the degree of saturation (or coagulation value) of the casting solution.

A new approach to the preparation of membranes with a desired structure and performance was proposed. Membranes with a nice spongy structure and high performance ($J \geq 100 \text{ l/m}^2\text{h}$) were obtained from casting solutions which located near the binodal line and PV of NSA $\geq 250 \text{ g/dL}$. The highest PWF ($J \geq 200 \text{ l/m}^2\text{h}$) corresponds to membranes obtained from a casting solutions with $\alpha^*=0.52-0.81$. However, in this case large-size macrovoids are dominant in the structure of membranes.

Table 2

Surface parameters of PES membranes prepared by using NSA with different PV.

PV of NSA, g/dL	Ra (nm)	Rq (nm)
37.9	6.4	8.2
50.4	10.2	13.2
78.3	34.5	42.5
750	41.9	58.0

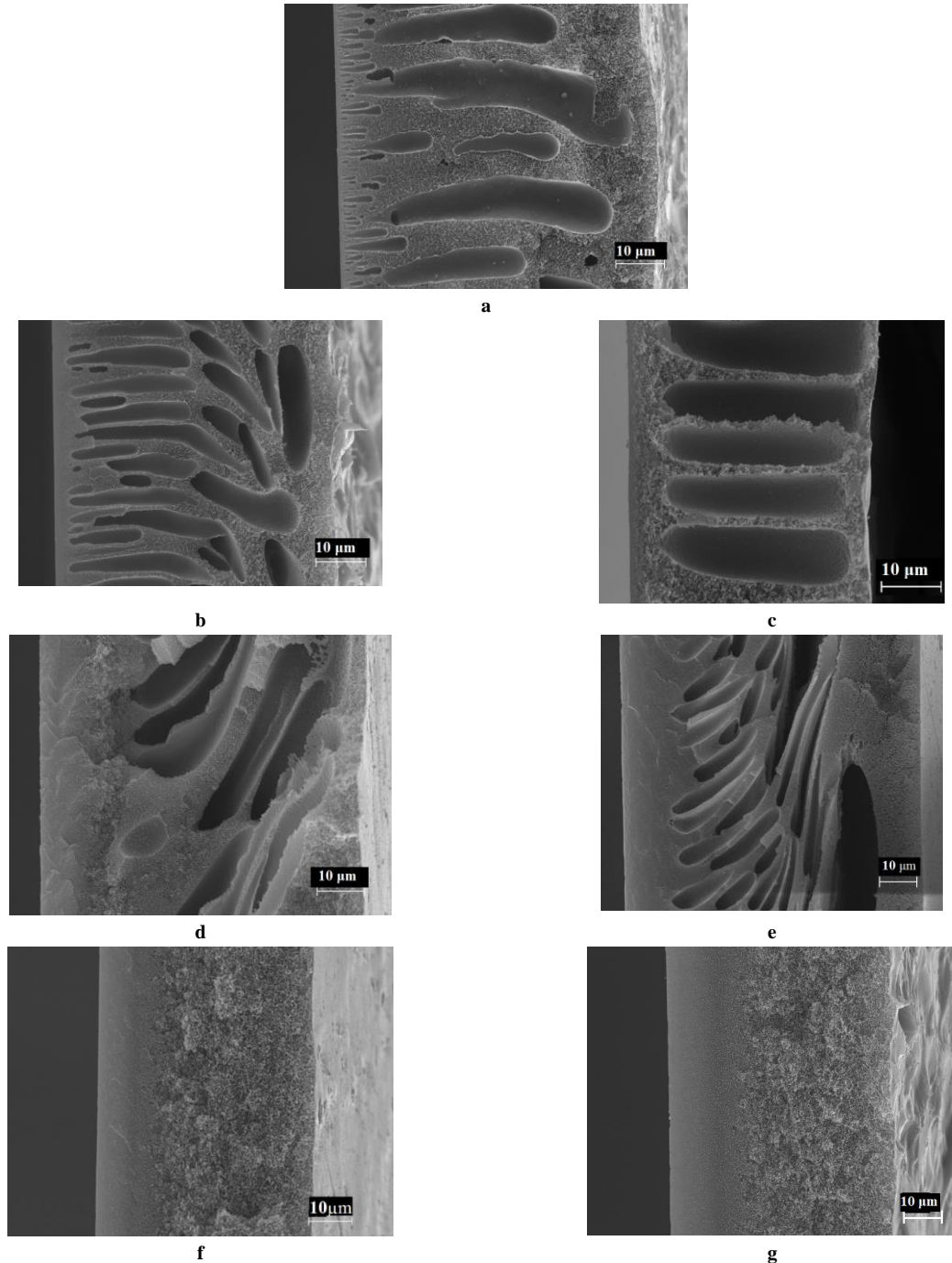


Fig. 9. Scanning electron micrographs of the cross section of PES membranes prepared from a casting solutions with PEG-400/Glycerol mixtures with different degree of saturation (α^*) and PV: a – $\alpha^*=0$; b – $\alpha^*=0.36$ PV=78.3 g/dL; c – $\alpha^*=0.35$ PV=750 g/dL; d – $\alpha^*=0.72$ PV=78.3 g/dL; e – $\alpha^*=0.71$ PV=750 g/dL; f – $\alpha^*=0.94$ PV=78.3 g/dL; g – $\alpha^*=0.94$ PV=750 g/dL.

Acknowledgements

This work was supported by Belarusian Republican Foundation for Fundamental Research, grant No. X18M-044.

Abbreviations

CV	coagulation value, g·dL ⁻¹
DMAC	<i>N,N</i> -dimethylacetamide
EIPS	evaporation induced phase separation
NIPS	non-solvent induced phase separation
NSA	non-solvent additive
PEG	polyethylene glycol
PES	polyethersulfone
PV	precipitation value
TIPS	thermally induced phase separation
VIPS	vapor induced phase separation

References

- [1] M. Mulder, Basic Principles of Membrane Technology, Kluwer Academic Publishers, Netherlands, 1996.
- [2] J.T. Jung, J.F. Kim, H.H. Wang, E. di Nicolo, E. Drioli, Y.M. Lee, Understanding the non-solvent induced phase separation (NIPS) effect during the fabrication of microporous PVDF membranes via thermally induced phase separation (TIPS), *J. Membr. Sci.* 514 (2016) 250–263. Doi:10.1016/j.memsci.2016.04.069
- [3] J. Barzin, B. Sadatnia, Correlation between macrovoid formation and the ternary phase diagram for polyethersulfone membranes prepared from two nearly similar solvents, *J. Membr. Sci.* 325 (2016) 92–97. Doi:10.1016/j.memsci.2008.07.003
- [4] D.J. Miller, D.J. Dreyer, C.W. Bielawski, D.R. Paul, B.D. Freeman, Surface modification of water purification membranes: a review, *Angew. Chem.* 56 (2017) 4662–4711. Doi:10.1002/anie.201601509
- [5] G. Arthanareeswaran, V.M. Starov, Effect of solvents on performance of polyethersulfone ultrafiltration membranes: Investigation of metal ion separations, *Desalination* 267 (2011) 57–63. Doi:10.1016/j.desal.2010.09.006
- [6] Y. Liu, G.H. Koops, H. Strathmann, Characterization of morphology controlled polyethersulfone hollow fiber membranes by the addition of polyethylene glycol to the dope and bore liquid solution, *J. Membr. Sci.* 223 (2003) 187–199. Doi:10.1016/S0376-7388(03)00322-3
- [7] A.K. Holda, I.F.J. Vankelecom, Understanding and guiding the phase inversion process for synthesis of solvent resistant nanofiltration membranes, *J. Appl. Polym. Sci.* 132 (2015) 42130. Doi:10.1002/app.42130
- [8] M.A. Aroon, A.F. Ismail, M.M. Montazer-Rahmati, T. Matsuura, Morphology and permeation properties of polysulfone membranes for gas separation: Effects of non-solvent additives and co-solvent, *Sep. Purif. Technol.* 72 (2009) 194–202. Doi:10.1016/j.seppur.2010.02.009
- [9] I.-Ch. Kim, K.-H. Lee, Effect of poly(ethylene glycol) 200 on the formation of a polyetherimide asymmetric membrane and its performance in aqueous solvent mixture permeation, *J. Membr. Sci.* 230 (2004) 183–188. Doi:10.1016/j.memsci.2003.11.002
- [10] Z. Wang, J. Ma, The role of nonsolvent in-diffusion velocity in determining polymeric membrane morphology, *Desalination* 286 (2012) 69–79. Doi:10.1016/j.desal.2011.11.006
- [11] P.S.T. Machado, A.C. Habert, C.P. Borges, Membrane formation mechanism based on precipitation kinetics and membrane morphology: flat and hollow fiber polysulfone membranes, *J. Membr. Sci.* 155 (1999) 171–183. Doi:10.1016/S0376-7388(98)00266-X
- [12] I. Wang, J. Ditter, R. Morris, R. Kesting inventors; USF Filtration and Separations Group Inc. Highly asymmetric ultrafiltration membranes, US patent 5,958,989. 1999.
- [13] A. Idris, M.J. Norashikin, M.Y. Noordin, Synthesis, characterization and performance of asymmetric polyethersulfone (PES) ultrafiltration membranes with polyethylene glycol of different molecular weights as additives, *Desalination* 207 (2007) 324–339. Doi:10.1016/j.desal.2006.08.008
- [14] B. Chakrabarty, A.K. Ghoshal, M.K. Purkait, Effect of molecular weight of PEG on membrane morphology and transport properties, *J. Membr. Sci.* 309 (2008) 209–221. Doi:10.1016/j.memsci.2007.10.027
- [15] I. Wang, J. Ditter, R. Morris, R. Kesting inventors; USF Filtration and Separations Group Inc. Highly asymmetric ultrafiltration membranes, US patent 5,928,774. 1999.
- [16] H. Pang, H. Gong, M. Du, Q. Shen, Z. Chen, Effect of non-solvent additive concentration on CO₂ absorption performance of polyvinylidene fluoride hollow fiber membrane contactor, *Sep. Purif. Technol.* 191 (2018) 38–47. Doi:10.1016/j.seppur.2017.09.012
- [17] T. Wang, Ch. Zhao, P.Li, Y.Li, J. Wang, Effect of non-solvent additives on the morphology and separation performance of poly(*m*-phenylene isophthalamide) (PMIA) hollow fiber nanofiltration membrane, *Desalination* 365 (2015) 293–307. Doi:10.1016/j.desal.2015.03.016
- [18] J. Han, D. Yang, S. Zhang, X. Jian, Effects of dope compositions on the structure and performance of PPES hollow fiber ultrafiltration membranes, *J. Membr. Sci.* 345 (2009) 257–266. Doi:10.1016/j.memsci.2009.09.008
- [19] S.-J. Shin, J.-P. Kim, H.-J. Kim, J.-H. Jeon, B.-R. Min, Preparation and characterization of polyethersulfone microfiltration membranes by a 2-methoxyethanol additive, *Desalination* 186 (2005), 1–10. Doi:10.1016/j.desal.2005.03.092
- [20] V. Laninovich, Relationship between type of nonsolvent additive and properties of polyethersulfone membranes, *Desalination* 186 (2005), 39–46. Doi:10.1016/j.desal.2005.01.017
- [21] L. Zheng, Z. Wu, Y. Zhang, Y. Wei, J. Wang, Effect of non-solvent additives on the morphology, pore structure, and direct contact membrane distillation performance of PVDF-CTFE hydrophobic membranes, *J. Eng. Sci.* 45 (2016) 28–39. DOI:10.1016/j.jes.2015.09.023
- [22] J.M.A. Tan, S.-H. Noh, G. Chowdhury, T. Matsuura, Influence of surface tensions of solvent/nonsolvent mixtures in membrane casting solutions on the performance of poly(2,6-dimethyl-1,4-phenylene) oxide membranes for gas separation applications, *J. Membr. Sci.* 174 (2000) 225–230. Doi:10.1016/S0376-7388(00)00383-5
- [23] D. Wang, W.K. Teo, K. Li, Preparation and characterization of high-flux polysulfone hollow fiber gas separation membranes, *J. Membr. Sci.* 204 (2002) 247–256. Doi:10.1016/S0376-7388(02)00047-9
- [24] Y. Feng, G. Han, T.-S. Chung, M. Weber, N. Widjojo, C. Maletz, Effects of polyethylene glycol on membrane formation and properties of hydrophilic sulfonated polyphenylenesulfone (sPPSU) membranes, *J. Membr. Sci.* 531 (2017) 27–35. Doi:10.1016/j.memsci.2017.02.040
- [25] D. Wang, K. Li, W.K. Teo, Highly permeable polyethersulfone hollow fiber gas separation membranes prepared using water as non-solvent additive, *J. Membr. Sci.* 176 (2000) 147–158. Doi:10.1016/S0376-7388(00)00419-1
- [26] M. Sadrzadeh, S. Bhattacharjee, Rational design of phase inversion membranes by tailoring thermodynamics and kinetics of casting solution using polymer additives, *J. Membr. Sci.* 441 (2013) 31–44. Doi:10.1016/j.memsci.2013.04.009
- [27] L. Wang, Z. Li, J. Ren, S.-G. Li, C. Jiang, Preliminary studies on the gelation time of poly(ether sulfones) membrane-forming system with an elongation method, *J. Membr. Sci.* 275 (2006) 46–51. Doi:10.1016/j.memsci.2005.08.019
- [28] Z. Li, C. Jiang, Investigation into the rheological properties of PES/NMP/nonsolvent membrane-forming systems, *J. Appl. Polym. Sci.* 82 (2001) 283–291. Doi:10.1002/app.1850
- [29] J. Ren, Z. Li, F.-S. Wong, Membrane structure control of asymmetric BTDA-TDI/MDI (P84) co-polyimide membranes by phase inversion process, *J. Membr. Sci.* 241 (2004) 305–314. Doi:10.1016/j.memsci.2004.06.001
- [30] B. Torrestiana-Sanchez, R.I. Ortiz-Basurto, E. Brito-De La Fuenteb, Effect of nonsolvents on properties of spinning solutions and polyethersulfone hollow fiber ultrafiltration membranes, *J. Membr. Sci.* 152 (1999) 19–28. Doi:10.1016/S0376-7388(98)00172-0
- [31] D. Wang, K. Li, W.K. Teo, Polyethersulfone hollow fiber gas separation membranes prepared from NMP/alcohol solvent systems, *J. Membr. Sci.* 115 (1996) 85–108. Doi:10.1016/0376-7388(95)00312-6
- [32] D. Wang, K. Li, W.K. Teo, Relationship between mass ratio of nonsolvent – additive to solvent in membrane casting solution and its coagulation value, *J. Membr. Sci.* 98 (1995) 233–240. Doi:10.1016/0376-7388(94)00191-Z
- [33] D.Wang, K.Li, S.Sourirajan, W.K. Teo, Phase separation phenomena of polysulfone/solvent/organic nonsolvent and polyethersulfone/solvent/organic nonsolvent systems, *J. Appl. Polym. Sci.* 50 (1993), 1693 – 1700. Doi:10.1002/app.1993.070501003
- [34] S.A. Pratsenko, A.V.Bilyukevich, Structure of casting solutions and its effect on the characteristics of polyamide membranes, *Polym. Sci. Ser. A, T.* 36, 3 (1994) 457–460.
- [35] H.A. Tsai, M.J. Hong, G.S. Huang, Y.C. Wang, C.L. Li, K.R. Lee, J.Y. Lai, Effect of DGDE additive on the morphology and pervaporation performances of asymmetric PSf hollow fiber membranes, *J. Membr. Sci.* 208 (2002) 233–245. Doi:10.1016/S0376-7388(02)00265-X
- [36] A.V. Bilyukevich, S.A. Pratsenko, T.V. Plisko, Influence of pore forming additives on properties of polyethersulfone membranes, *Khimicheskaya Tekhnologiya*, 3(2012)174–179.
- [37] J.-Y. Lai, F.-C. Lin, C.-C. Wang, D.-M. Wang, Effect of nonsolvent additives on the porosity and morphology of asymmetric TPX membranes, *J. Membr. Sci.* 118 (1996) 49–61. Doi:10.1016/0376-7388(96)00084-1
- [38] L.-W. Chen, T.-H. Young, Effect of nonsolvents on the mechanism of wet-casting membrane formation from EVAL copolymers, *J. Membr. Sci.* 59 (1991) 15–26. Doi:10.1016/S0376-7388(00)81218-1
- [39] C.W. Yao, R.P. Burford, A.G. Fane, C.J.D. Fell, Effect of coagulation conditions on structure and properties of membranes from aliphatic polyamides, *J. Membr. Sci.* 38 (1988) 113–125. Doi:10.1016/S0376-7388(00)80874-1
- [40] K.-Y. Chun, S.-H. Jang, H.-S. Kim, Y.-W. Kim, H.-S. Han, Effects of solvent on the pore formation in asymmetric 6FDA–4,4'ODA polyimide membrane: terms of thermodynamics, precipitation kinetics, and physical factors, *J. Membr. Sci.* 169 (2000) 197–204. Doi:10.1016/S0376-7388(99)00336-1
- [41] S.P. Papkov, Physicochemical bases of processing of polymer solutions, Chemistry, Moscow, 1971.
- [42] A. Ziabicki, Fundamentals of Fiber Formation: The Science of Fiber Spinning and Drawing, John Wiley & Sons, London, 1976.
- [43] L. Zheng, J. Wang, D. Yu, Y. Zhang, Y. Wei, Preparation of PVDF-CTFE

- hydrophobic membrane by non-solvent induced phase inversion: Relation between polymorphism and phase inversion, *J. Membr. Sci.* 550 (2018) 480-491. Doi:10.1016/j.memsci.2018.01.013
- [44] T.V. Plisko, A.V. Bilyukevich, Y.A. Karslyan, A.A. Ovcharova, V.V. Volkov, Development of high flux ultrafiltration polyphenylsulfone membranes applying the systems with upper and lower critical solution temperatures: Effect of polyethylene glycol molecular weight and coagulation bath temperature, *J. Membr. Sci.* 565 (2018) 266-280. Doi:10.1016/j.memsci.2018.08.038
- [45] A.A. Tager, G.O. Botvinnik, Viscous flow activation parameters and structure of concentrated polymer solutions, *Polymer Science*. 26A №6 (1974) 1284-1288.
- [46] M.-J. Han, S.-T. Nam, Thermodynamic and rheological variation in polysulfone solution by PVP and its effect on the preparation of phase inversion membrane, *J. Membr. Sci.* 202 (2002) 55-61. Doi:10.1016/S0376-7388(01)00718-9
- [47] H. Ohya, S. Shiki, H. Kawakami, Fabrication study of polysulfone hollow-fiber microfiltration membranes: optimal dope viscosity for nucleation and growth, *J. Membr. Sci.* 326 (2009) 293-302. Doi:10.1016/j.memsci.2008.10.001
- [48] J.-H. Kim, K.-H. Lee, Effect of PEG additive on membrane formation by phase inversion, *J. Membr. Sci.* 138 (1998) 153-163. Doi:10.1016/S0376-7388(97)00224-X
- [49] M.K. Sinha, M.K. Purkait, Enhancement of hydrophilicity of poly(vinylidene fluoride-co-hexafluoropropylene) (PVDF-HFP) membrane using various alcohols as nonsolvent additives, *Desalination*. 338 (2014) 106-114. Doi:10.1016/j.desal.2014.02.002